

# CCR5 blockage by maraviroc induces cytotoxic and apoptotic effects in colorectal cancer cells

Asim Pervaiz<sup>1</sup> · Shariq Ansari<sup>1</sup> · Martin R. Berger<sup>1</sup> · Hassan Adwan<sup>1,2</sup>

Received: 5 March 2015 / Accepted: 26 March 2015 / Published online: 4 April 2015  
© Springer Science+Business Media New York 2015

**Abstract** Alterations in the expression of C–C chemokine receptor type 5 (*CCR5* or *CD195*) have been correlated with disease progression in different cancers. Recently, a few investigations have reported the blockage of this receptor by an antagonist (maraviroc) and its antineoplastic effects on tumor cell growth. However, little is known about the mechanistic reasons behind these antineoplastic effects of *CCR5* blockage by maraviroc. In this study, we blocked the *CCR5* receptor by maraviroc in SW480 and SW620 colorectal cancer cells to study the resulting changes in biological properties and related pathways. This blockage induced significantly reduced proliferation and a profound arrest in G1 phase of the cell cycle. Concomitantly, maraviroc caused significant signs of apoptosis at morphological level. Significant modulation of multiple apoptosis-relevant genes was also noticed at mRNA levels. In addition, we found remarkable increases in cleaved caspases at protein level. These modulations led us to propose a signaling pathway for the observed apoptotic effects. In conclusion, blocking the *CCR5* by maraviroc induces significant cytotoxic and apoptotic effects in colorectal cancer cells. Thus, maraviroc can be considered a model compound, which may foster the development of further *CCR5* antagonists to be used for the treatment of colorectal cancer.

**Keywords** C–C chemokine receptor type 5 · Maraviroc · SW480 · SW620 · Caspases activation · Apoptosis induction

## Introduction

Chemokines are small secretory chemo-attractant cytokines (8–14 kDa), which mainly regulate the directional migration of leukocytes, epithelial and endothelial cells in a concentration-dependent manner [1, 2]. The whole chemokine network is comprised of about 50 ligands and 20 receptors, where they demonstrate a phenomenon of redundancy as multiple chemokine ligands can interact with a single receptor and multiple receptors could be the target of a single chemokine ligand [3–5]. High levels of inflammatory cytokines, hypoxia, polarization/differentiation of immune cells and production of various growth factors can induce expressional changes of chemokines [6–8]. The expression patterns of the chemokine network are of vital importance in different autoimmune diseases, pathogenic situations, tumorigenesis and metastasis of malignant cancers [8, 9]. Significant alterations in the expressional profile of chemokine ligands and their corresponding receptors have been observed in different human cancers, which, in turn, alter the immune response and effect the progression of tumor mass [10, 11]. Nevertheless, the final outcomes of these modulations depend on the type of chemokines involved, cancerous tissue, leukocyte infiltrate and surrounding microenvironment [12, 13].

Colorectal cancer (CRC) is the third leading type of cancer in the developed countries and the second major cause of cancer-related mortalities worldwide [14, 15]. Significant alterations in the chemokines and their corresponding effects on disease progression have been

**Electronic supplementary material** The online version of this article (doi:10.1007/s12032-015-0607-x) contains supplementary material, which is available to authorized users.

✉ Martin R. Berger  
m.berger@dkfz-heidelberg.de

<sup>1</sup> Toxicology and Chemotherapy Unit, German Cancer Research Center, Im Neuenheimer Feld 581, 69120 Heidelberg, Germany

<sup>2</sup> Present Address: German University of Cairo, Cairo, Egypt

identified in primary and metastatic CRC. Being an important component of chemokine network, understanding the role of chemokine receptor 5 (*CCR5*) in CRC is of paramount importance. *CCR5* is a well-characterized chemokine receptor, which was identified for the first time about two decades ago [16, 17]. Three chemokine ligands for this receptor, described in detail, are CCL3 (MIP-1 $\alpha$ ), CCL4 (MIP-1 $\beta$ ) and CCL5 (RANTES). *CCR5* is a G-protein-coupled receptor with seven transmembrane loops, which interacts with the corresponding ligands and activates the intracellular bound heterotrimeric G $\alpha\beta\gamma$  unit for subsequent downstream signaling [18, 19]. Noteworthy alterations in the expression of *CCR5* have been correlated with the prognosis of primary CRC including metastasis to potential target organs. Regarding the expression level of *CCR5* on CRC cells, contradicting reports have been published. Some authors reported higher *CCR5* expression in primary CRC with increased local growth [20, 21], while others have found that high *CCR5* expression is required for metastasis [22, 23]. In addition to this, it is presumed that variations in expressional pattern of *CCR5* can alter the immune response system in CRC, which in turn will favor the further progression of the disease [24–28].

In the present study, we aimed at investigating the role of *CCR5* receptor in CRC cell lines following its blockage with an available antagonist. For this purpose, we selected primary (SW480) and metastatic (SW620) human CRC cell lines for detecting possible differences between primary and metastatic CRC malignancies. *CCR5* receptor was blocked by maraviroc (MVC), which is a FDA-approved antagonist for this receptor [29]. Following the blockage of *CCR5* by MVC, we investigated the impact on cellular proliferation, cell cycle distributions and apoptosis-related activities/pathways in the selected cell lines. This study illustrates the systematic impact of blocking *CCR5* on various biological properties of CRC cells. Furthermore, the results led us to search into the importance of this receptor as a therapeutic for treatment of CRC.

## Materials and methods

### Cell lines

Two human colon adenocarcinoma cell lines, SW480 (primary) and SW620 (metastatic), were obtained from American Type Culture Collection (ATCC) and cultured in RPMI-1640 medium (Invitrogen, Darmstadt, Germany) supplemented with fetal bovine serum (10 %) and L-glutamine (2 mM). The cell lines, free of pathogenic contaminations, were maintained under standard incubation conditions (5 % CO<sub>2</sub>, 37 °C) with a humidified atmosphere and passaged routinely to maintain the logarithmically growing cell populations.

### Cell viability assay

Viability of selected cell lines, following the treatment with MVC (UK-427857, Selleck Chemical Co. China), was assessed by MTT (3-[4,5-dimethylthiazol-2-yl]-2,5-diphenyltetrazolium bromide) dye reduction assay. In brief, the cells were seeded at pre-optimized density ( $5 \times 10^3$  cells/well) in 96-well plates and treated with increasing concentrations of MVC (1–750  $\mu$ M) for three time points (24, 48 and 72 h). Surviving cell fractions from the treated and control groups (eight replicates/sample) were determined by adding 10  $\mu$ l/well MTT solution (10 mg/ml in PBS) and dissolving newly formed formazan crystals with 100  $\mu$ l of acidic 2-propanol (0.04 N HCl). Optical density was measured by an ELISA plate reader (Anthos Mikrosysteme GmbH, Krefeld, Germany) at 540 nm wavelength with 690-nm reference filter. Cell survival rates were calculated as the percentages of untreated controls, and inhibitory concentrations (IC) were determined by GraphPad Prism 5 software.

### Cell cycle assay

Effects of antagonizing *CCR5* by MVC on cell cycle were determined by propidium iodide (PI) fluorescent staining and flow cytometry analysis (FACS). Briefly, the cells were seeded ( $3.5 \times 10^5$  cells/flask) in 25-cm<sup>2</sup> cell culture flasks and treated with MVC (IC<sub>25</sub>, IC<sub>50</sub> or IC<sub>75</sub>). After 48 h of drug exposure, the cells were harvested and re-suspended in 0.1 ml of PBS ( $2 \times 10^5$  cells) followed by the addition of ice-cold ethanol (70 %) for fixation. After an incubation period of 2 h at 4 °C, the cells were washed, re-suspended in PBS containing RNaseA (1 mg/ml) to digest their RNA and incubated for 30 min at 37 °C. Afterwards, PI (50  $\mu$ g/ml) was added to the cells, and analysis was done immediately ( $\leq 30$  min) in a FACS Canto (BD Biosciences, San Jose, CA, USA). Ten thousand cells (events) were analyzed from each sample, and the cell's distributions in G<sub>0</sub>/G<sub>1</sub>, S and G<sub>2</sub>/M phases of cell cycle were calculated by ModFit LT software.

### Hoechst 33324 staining

The cells were seeded ( $1.5 \times 10^5$  cells/well) in 6-well plates having sterilized cover slips inside. Next day, treatment was done with increasing concentrations of MVC (IC<sub>25</sub>, IC<sub>50</sub> or IC<sub>75</sub>) for 48 h followed by the fixation of cells with 4 % formaldehyde and permeabilization with 0.3 % Triton X-100 (Sigma, Munich, Germany). Then, the cells were stained with 1.6 mM Hoechst 33342 dye (Invitrogen, Karlsruhe Germany), placed top down on glass slides and kept in the dark until analyses. Prepared slides were randomly photographed with a fluorescence Axiophot microscope (Carl Zeiss, Oberkochen, Germany).

### Annexin V-FITC flow cytometry assay

Early signs of apoptosis, in response to MVC treatment, were investigated by Annexin V-FITC Apoptosis Detection Kit (*eBioscience, Frankfurt, Germany*). In brief,  $3.5 \times 10^5$  cells/flask were seeded in 25-cm<sup>2</sup> cell culture flasks and next day treated with MVC (IC<sub>25</sub>, IC<sub>50</sub> or IC<sub>75</sub>) for 48 h. The cells were harvested with EDTA free trypsin (0.25 %) and washed with PBS followed by a second wash with 1X binding buffer provided with the kit. Then,  $2 \times 10^5$  cells were re-suspended in 100 µl of 1X binding buffer, and 5 µl of fluorochrome-conjugated Annexin V dye was added before samples were incubated for 15 min at room temperature in dark. After the incubation period, the cells were washed again with 1X binding buffer to remove additional unbound Annexin V dye and re-suspended in 200 µl of 1X binding buffer. PI (5 µl), provided along the kit, was added to each sample, and analyses was done with a FACSCalibur flow cytometer (BD Biosciences, San Jose, CA, USA).

### RNA isolation and cDNA synthesis

The CRC cells were seeded in 6-well plates ( $1.5 \times 10^5$  cells/well) and treated with MVC (IC<sub>25</sub>, IC<sub>50</sub> or IC<sub>75</sub>) on next day. After 48 h of drug exposure, the cells were harvested and washed and total RNA was extracted from the cell pellets with RNeasy Mini kit (Qiagen, Hilden, Germany) following the manufacturer's protocol. Concentrations of the extracted RNA were measured by a GeneQuant *pro* spectrophotometer (GE Healthcare, Munich, Germany), and 1 µg RNA was used to synthesize complementary DNA (cDNA) by using Maxima reverse transcriptase enzyme (Thermo Scientific, Schwerte, Germany). Prepared cDNA samples were used in the subsequent real-time PCR analysis.

### Quantitative real-time RT-PCR

Modulation of mRNA expression in response to blocking *CCR5* with MVC was studied for cell cycle-relevant genes (cyclins) by qRT-PCR methodology in both selected cell lines. For this purpose, the cDNA samples were subjected to qRT-PCR amplification by using 2X LC480 Master Mix along with the appropriate probes from the Human Universal Probe library (Roche, Mannheim, Germany). The samples were amplified in triplicate, and the expression level of a reference gene (GAPDH) was used for normalizing the data. After the amplification procedures, fold changes were calculated by the  $2^{-\Delta\Delta CT}$  method [30]. Primer sequences used for the amplifications of cyclins and GAPDH are shown in Supplementary Table 1.

### Human apoptosis panel, 96

To have a deeper insight about the effects of MVC on apoptosis-related genes, we used a ready-made *Human Apoptosis Panel, 96* (Roche, Mannheim, Germany). This panel included the primers for 84 apoptosis-relevant genes along with their corresponding probes. In addition to this, two RT-negative controls to monitor the residual genomic DNA from RNA extraction step, three RT-positive controls to check the quality of reverse transcription and seven reference genes for normalization of the data were also included in this panel. For this analysis, SW480 cells were exposed to increasing concentrations of MVC (IC<sub>50</sub> and IC<sub>75</sub>) for 48 h, followed by extraction of total RNA and cDNA synthesis as described above. RT-PCR was performed by adding 0.5 µl cDNA/sample (50 µl transcribed from 2.5 µg extracted RNA) along with 2X LC480 Master Mix (Roche, Mannheim, Germany) in a LightCycler 480 Real-Time PCR System.

### Western blot analysis

The two cell lines ( $3 \times 10^5$  cells/flask) were treated in 25-cm<sup>2</sup> cell culture flasks with MVC (IC<sub>25</sub>, IC<sub>50</sub> or IC<sub>75</sub>) for 48 h. After the treatment, cells were harvested, transferred to 1.5-ml microcentrifuge tubes and washed in PBS and pellets were lysed with RIPA buffer (150 mM sodium chloride, 1.0 % NP-40, 0.5 % sodium deoxycholate, 0.1 % sodium dodecyl sulfate, 50 mM Tris, pH 8.0) and supplemented with complete protease inhibitor cocktail tablets (Roche, Mannheim, Germany). The lysates were maintained at constant agitation for 30 min at 4 °C, and later the supernatant was collected after spinning at 14,000 rpm at 4 °C for 20 min. The supernatant was quantified for protein concentration using the Pierce Protein Assay. The total protein lysates (30–50 µg) were subjected to electrophoresis on 4–12 % gradient polyacrylamide SDS gels. Proteins were transferred onto PVDF membranes, and the membranes were probed for different proteins (cleaved PARP, cleaved caspase 3, cleaved caspase 7 and cleaved caspase 9) using specific antibodies (Cell Signaling Technologies, Frankfurt, Germany) as per manufacturer's instructions. Immunoblots were developed using a HRP-conjugated anti-mouse or anti-rabbit IgG (Cell Signaling Technologies, Frankfurt, Germany) and ECL-System (Amersham Pharmacia Biotech, Munich, Germany). Levels of β-actin were used to normalize the protein expression. Relative concentrations were assessed by densitometric analysis of digitized autographic images using the ImageJ Program.

## Results

### Blocking the *CCR5* induces cytotoxicity in CRC cells

SW480 and SW620 cells were treated with increasing concentrations of MVC (1–750  $\mu\text{M}$ ), and resulting effects on cell viability were investigated by MTT dye reduction assay. MVC reduced the cell proliferation and led to cytotoxic effects in a concentration-dependent manner in both cell lines. At lower concentrations of MVC ( $\leq 50 \mu\text{M}$ ), there were stimulatory effects on cell proliferation, while above 100  $\mu\text{M}$  concentrations, inhibitory effects were found as calculated by GraphPad Prism 5 software. Concentrations from 100 to 750  $\mu\text{M}$  caused a steady decline in survival rates for both cell lines in a dose–response curve.  $\text{IC}_{50}$  values, with 95 % confidence limits, were calculated for both cell lines for the three time points (Fig. 1).

### Maraviroc induces significant arrest in G1 phase of the cell cycle

Both CRC cell lines were analyzed after treatment with MVC to see the effects of *CCR5* blockage on cell cycle. In the control samples, both cell lines illustrated comparable and almost equal distributions in G0/G1 (51–54 %) and S phase (44–45 %) cells as well as significant lower

percentages of G2/M phase cells (2–4 %). In response to MVC exposure, both cell lines showed an increase in G0/G1 fractions, followed by a subsequent decrease in S phase cells. The effects were more profound in SW620 cells, where maximum increase in G0/G1 phase was 16 % as compared to 3 % in SW480 cells. With regard to S phase, both cell lines demonstrated a decrease in cell's % in a concentration-dependent format as shown by a maximum reduction of 5 and 18 % for SW480 and SW620 cells, respectively. In response to the  $\text{IC}_{75}$  concentrations of MVC, a mild G2/M phase arrest was observed as shown by an increase of 5 and 2 % for SW480 and SW620 cells, respectively (Fig. 2).

### *CCR5* blockage modulates the expression of cyclins

Modulations in different phases of cell cycle provided us the base to investigate expressional profiles of the cell cycle-relevant genes (cyclins). For this purpose, after treatment with MVC ( $\text{IC}_{25}$ ,  $\text{IC}_{50}$  or  $\text{IC}_{75}$ ), we studied the expression patterns of cyclin family genes at mRNA level by qPCR. Following normalization of the results, we noticed a consistent, concentration-dependent down-regulation of cyclin D1 (*CCND1*) for SW480 cells (maximum  $-2.69$ -fold), while SW620 cells showed a moderate down-regulation of *CCND1* (maximum  $-1.45$ -fold) with higher

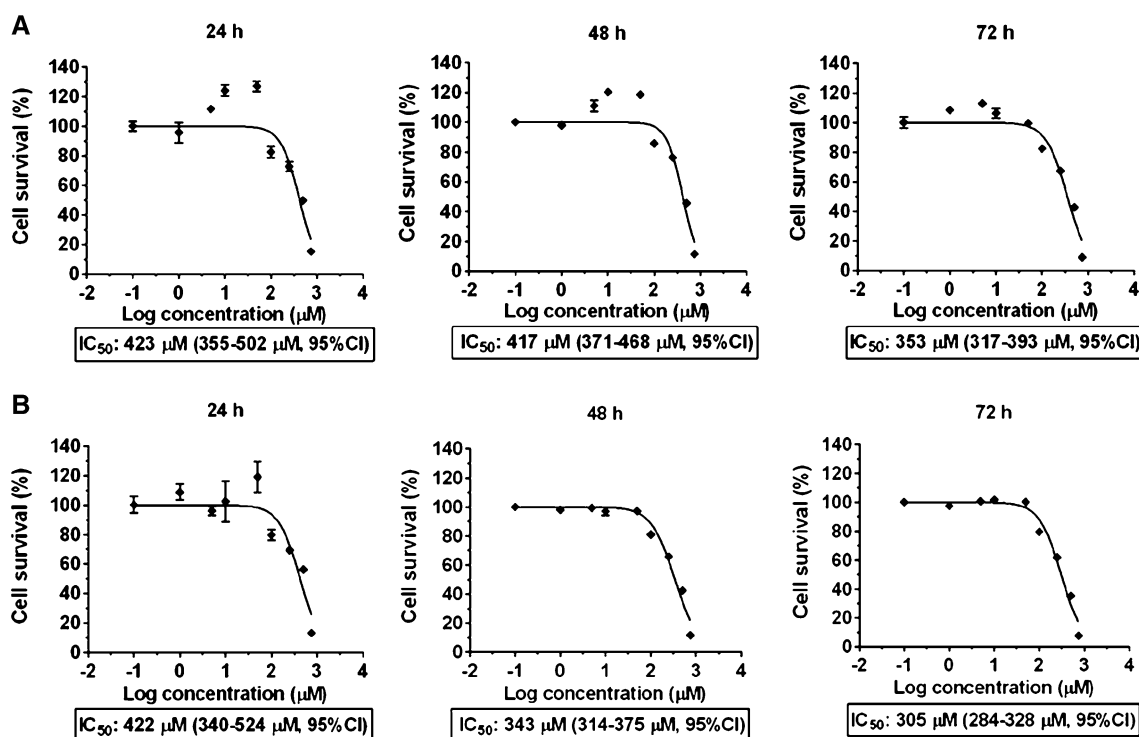


**Fig. 1** In vitro cytotoxic effects induced by maraviroc in colorectal cancer cells: **a**, **b** SW480 and SW620 cells, respectively, were treated with 1–750  $\mu\text{M}$  of maraviroc for 24, 48 and 72 h. Cytotoxicity was

measured by MTT dye reduction assay.  $\text{IC}_{50}$  values with 95 % confidence limits are given below the respective curves

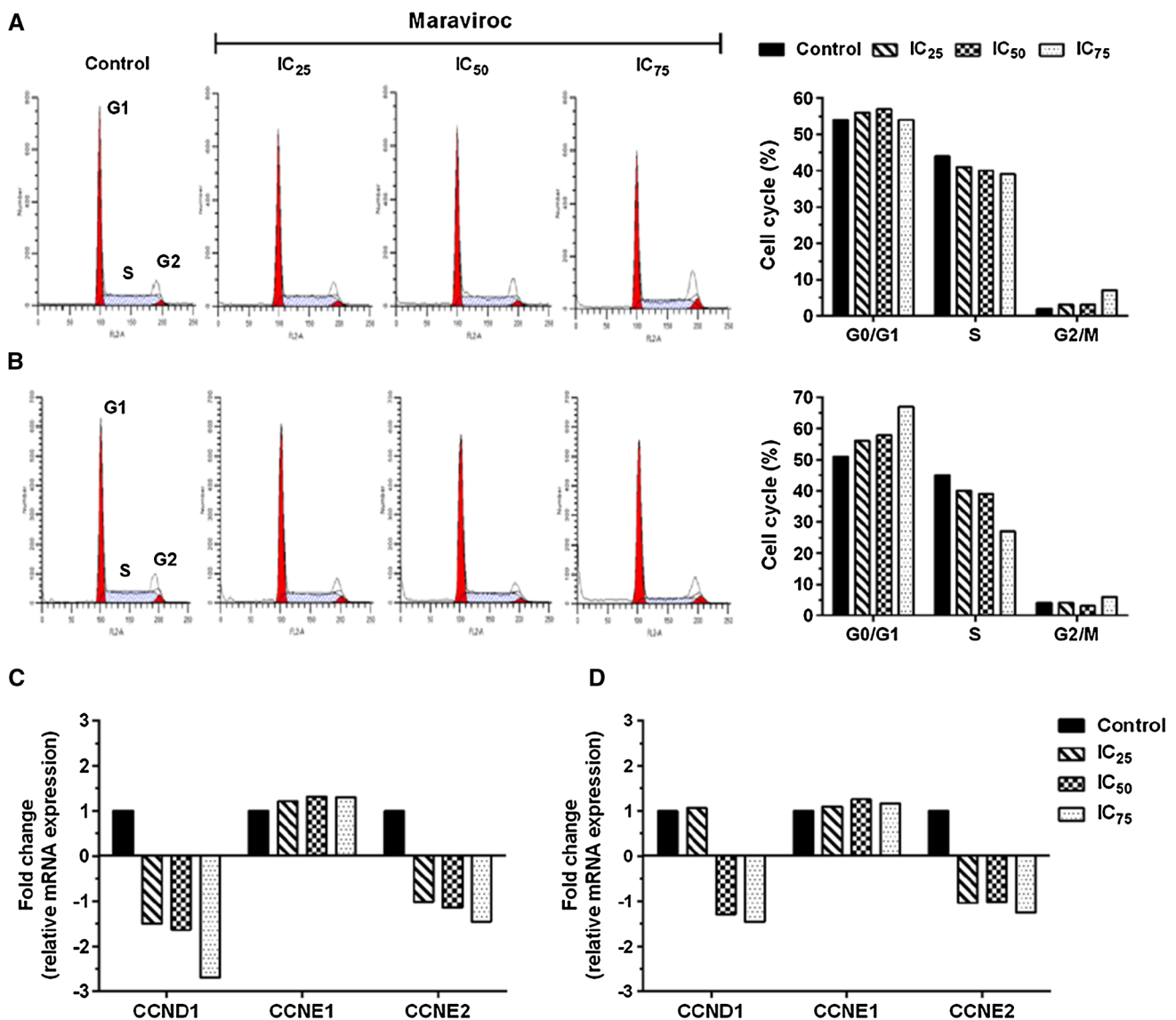


**Fig. 2** Effects of maraviroc on cell cycle: **a, b** SW480 and SW620 cells, respectively, show G1 phase arrest at lower maraviroc concentrations (IC<sub>25</sub>, IC<sub>50</sub>), while additional G2 arrest is visible at higher concentrations (IC<sub>75</sub>). **c, d** In SW480 and SW620 cells,

respectively, expression levels of CCND1 and CCNE2 were down-regulated concentration dependently (except for IC<sub>25</sub> concentration in SW620 cells), while CCNE1 was slightly up-regulated

concentrations of MVC (IC<sub>75</sub>). Both selected cell lines illustrated slight induction of cyclin E1 (CCNE1) and inhibition of cyclin E2 (CCNE2) as shown by a maximum change of 1.32- and -1.46-fold, respectively (Fig. 2).

concentrations of the *CCR5* antagonist (IC<sub>25</sub>), chromatin condensation was observed, while at higher concentrations (IC<sub>50</sub> and IC<sub>75</sub>), significant nuclear shrinkage and fragmentation were also noticed (Fig. 3).

**Nuclear/DNA fragmentation by maraviroc**

**CCR5 blockage by maraviroc stimulates apoptosis**

To determine whether the *CCR5* blockage exerts any apoptotic activities at morphological level, we studied the ability of MVC to induce oligonucleosomal DNA/nuclear fragmentation in the selected cell lines. Exposure of both cell lines to increasing concentrations of MVC (IC<sub>25</sub>-IC<sub>75</sub>) for 48 h led to disruptive changes in nuclei. At lower

Destructive morphological changes in the nuclei/DNA by MVC led to further investigations about apoptosis induction by *CCR5* blockage. For this purpose, following treatment with MVC, we examined annexin V-FITC-based labeling of the inner membrane-bound phosphatidylserine (PS) of the cells. Both cell lines showed a significant



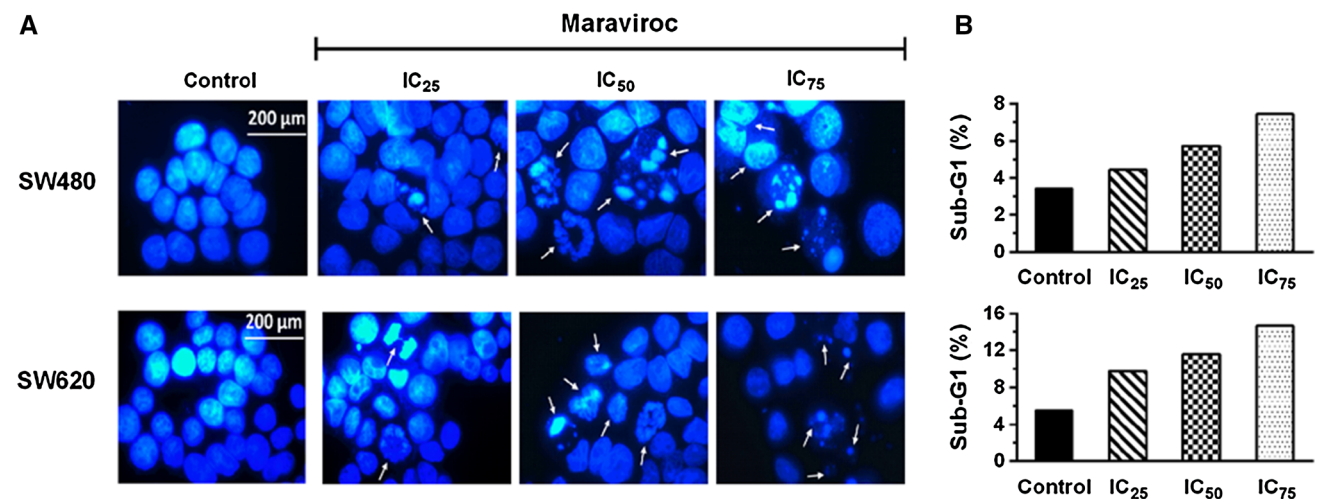


**Fig. 3** Morphological signs of apoptosis in colorectal cancer cells treated with maraviroc: **a** Nuclear shrinkage, chromatin condensation and fragmentation (indicated by white arrows) are visible in SW480 and SW620 cells treated with increasing concentrations of maraviroc

and subsequent staining with Hoechst 33342. **b** Corresponding sub-G1 (hypodiploid) DNA fractions obtained from flow cytometry analysis after the treatment with maraviroc are shown

increase in annexin V-positive cells with increasing concentrations of MVC as shown in Fig. 4. Maximum increases in annexin V-positive cells, in response to the highest concentrations of MVC (IC<sub>75</sub>), were 27 and 24 % for SW480 and SW620 cells, respectively. The continuous increase in the percentages of annexin V-bound cells in a concentration-dependent format showed the ability of MVC to induce apoptosis in CRC cell lines. Furthermore, the steady increase in apoptotic cells corroborated our cytotoxicity and nuclei/DNA fragmentation data from MTT and Hoechst 33342 staining assays, respectively.

#### Maraviroc induces multiple apoptosis-relevant genes

To figure out mechanistic aspects of *CCR5* blockage by MVC and its correlation with apoptotic effects, we investigated the apoptosis-relevant genes by a ready-made apoptosis panel (see materials and methods). SW480 cells, treated with two different concentrations of MVC (IC<sub>50</sub> and IC<sub>75</sub>), showed significant induction ( $\geq$ twofold) of 15 pro- and anti-apoptosis-relevant genes at mRNA level. Out of the 84 genes included in this panel, 68 genes were not altered significantly ( $\leq$ twofold), while one gene (NGFR) was down-regulated to a maximum fourfold. Nevertheless, significant induction was observed in a variety of gene families like caspases (1, 4, 5 and 10), stress-related BCL2 family (BCL2, BBC3, BIRC3 and BCL2L10) and death receptor signaling molecules (FAS, FASLG, TNF, TNFRSF1A, TNFRSF25) as shown in Fig. 5a. In addition to this, based on the results from the apoptosis panel, a signaling pathway for apoptosis was predicted by using the

*Ingenuity Software* (Redwood, CA, USA) as shown in Fig. 5b.

#### Activation of cleaved caspases by maraviroc

To support and confirm the idea of induction of apoptosis in CRC cells by MVC exposure, we examined the expressional levels of caspases by western blot analysis. Both cell lines were exposed to varying concentrations of MVC (IC<sub>25</sub>, IC<sub>50</sub> or IC<sub>75</sub>) for 48 h, and expression levels of activated/cleaved caspases 3, 7, and 9 were examined at protein level. The three caspases, which regulate the final steps of apoptosis, showed significant boosts in expression after MVC treatment. The utmost increases in expressions for caspases 3, 7 and 9 were 4.9-, 8.6- and 2.5-fold for SW480 cells, whereas SW620 cells showed 51.8-, 7.1- and 2.1-fold inductions, respectively. In addition to this, expression levels of cleaved PARP protein, which is a key hallmark of apoptosis, were also found to be significantly elevated with a maximum induction of 4.3- and 17.6-fold for SW480 and SW620 cells, respectively (Fig. 6).

#### Discussion

MVC is the only clinically available and well-tolerated non-competitive (allosteric) *CCR5* antagonist, which has been used for the treatment of *CCR5*-dependant immunodeficiency virus type 1 (HIV-1) infection. In recent years, MVC was also assessed for its potential as antineoplastic agent in a variety of primary and metastatic cancers. In this regard, animal models have been used to study the impact

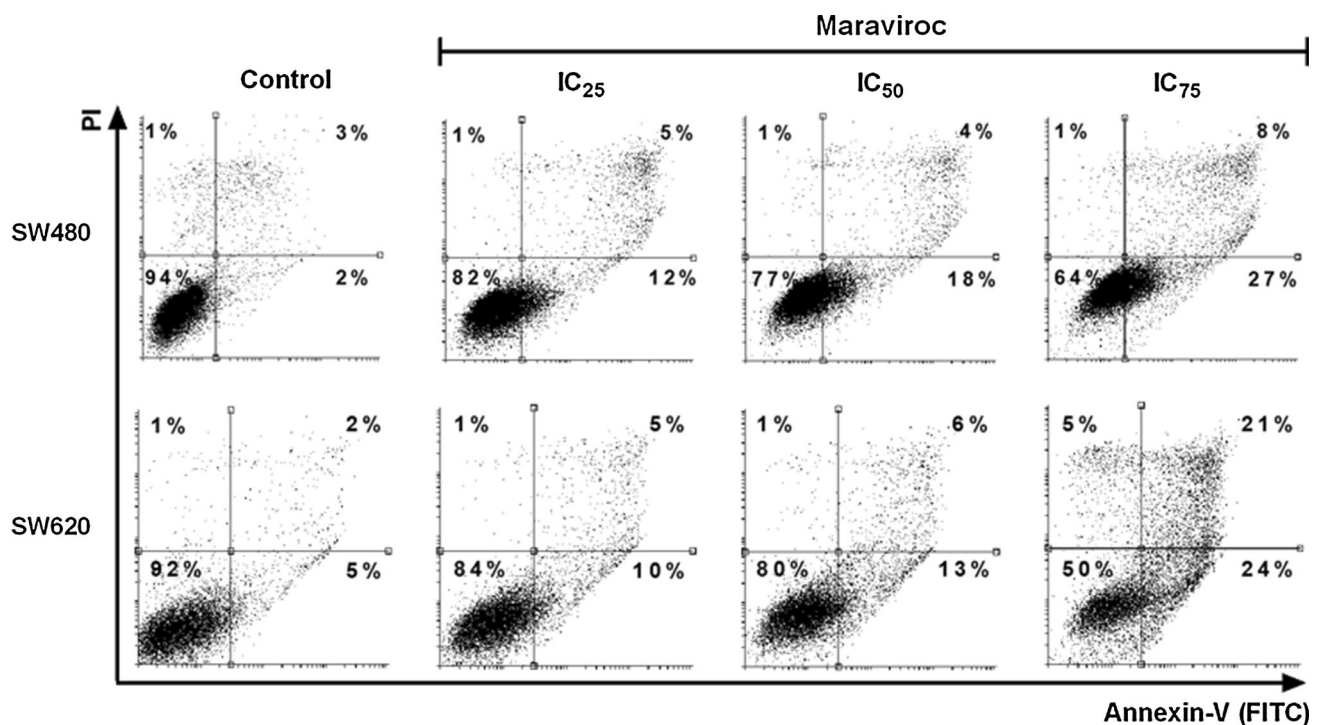


**Fig. 4** Effects of maraviroc on phosphatidylserine translocation. Induction of apoptosis in colorectal cancer cells by maraviroc exposure was examined by annexin V-FITC binding assay. Cells were treated with increasing concentrations of maraviroc for 48 h.

Concentration-dependent induction of early apoptosis was observed in both colorectal cancer cell lines as indicated by the corresponding percentages in *lower right* quadrants

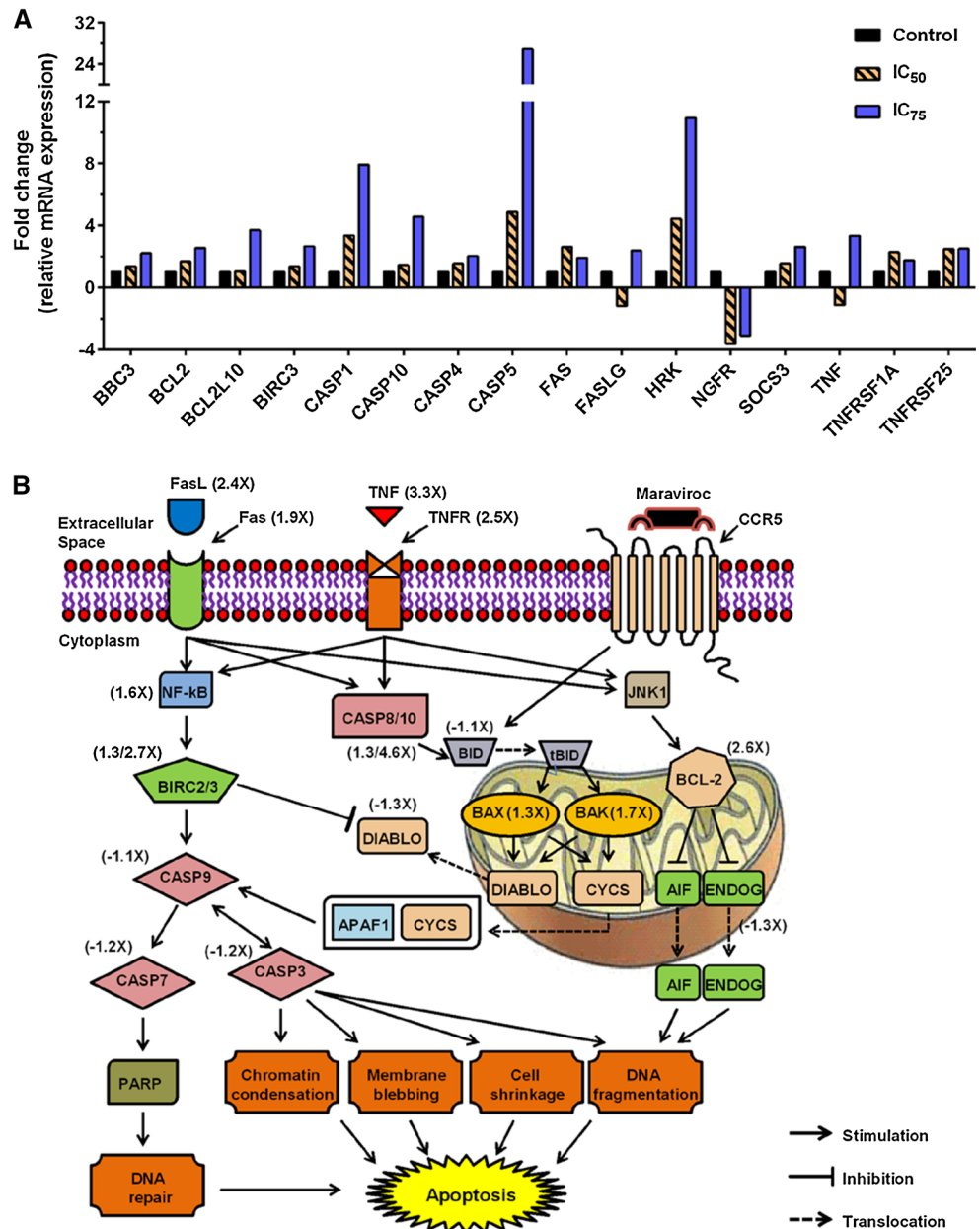
of *CCR5* blockage by MVC and subsequent effects on tumor progression [31–33]. Promising outcomes from these cancer-related studies (other than CRC) involving MVC as a *CCR5* blocker provoked us to study the effects of this antagonist in CRC cells.

In this study, we examined the role of *CCR5* in two CRC cell lines (SW480 and SW620) by blocking the receptor with MVC. In MTT assay, MVC exposure showed cytotoxic effects in both cell lines at higher concentrations ( $\geq 100 \mu\text{M}$ ), while there were initially some stimulatory effects at lower concentrations ( $\leq 50 \mu\text{M}$ ). Although, clinically used dosages of MVC are not associated with serum levels higher than  $100 \mu\text{M}$ , the antineoplastic success of MVC in mice-bearing breast, gastric or hepatocellular cancers indicates a potential of this drug in vivo [31–34]. We next aimed at finding the mechanism causing reduced cell proliferation in response to *CCR5* blockage by MVC. For this purpose, we studied the possible effects on cell cycle in CRC cells by PI staining and flow cytometry. MVC exposure resulted in G1 phase arrest in both CRC cell lines, and a G2 phase arrest was found only for the highest MVC concentrations (IC<sub>75</sub>). We focused at the major arrested G1 phase at molecular levels and noticed the inhibition of cell cycle-relevant genes in both cell lines. Most prominent down-regulation was observed for

*CCND1*, which interacts and regulates cyclin-dependent kinases (CDKs). In this regard, two important CDKs are CDK4 and CDK6, which are required for G1/S phase transition of the cell cycle [35, 36]. Thus, inhibition of *CCND1* by MVC exposure hypothetically led to the decreased activity of CDK4 and CDK6, which ultimately hampered G1/S phase transition leading to G1 phase arrest. In addition to this, we found a moderate inhibition of *CCNE2*, which predominantly interacts with CDK2 and also regulates the G1/S transition of the cell cycle [37].

We further studied the cytotoxic mechanisms resulting from *CCR5* blockage by MVC and found clear signs of apoptosis at morphological level. MVC induced the typical features of apoptosis like detachment of cells from the culture dish, blebbing, shrinkage in size and fragmentation of DNA/nuclei [38]. These signs of apoptosis, examined by general observations and staining protocols, were further studied by annexin V-FITC staining. Apoptosis is considered as programmed cell death, and one of the preliminary events in this process is translocation of membrane-bound PS molecules from the inner side of the plasma membrane to the outer surface [39]. Annexin V is a  $\text{Ca}^{2+}$ -dependent phospholipid binding protein and has high affinity to bind these exposed PS molecules. In response to increasing concentrations of MVC, there were profound and almost

**Fig. 5** Modulation of multiple apoptosis-related genes by maraviroc exposure: **a** SW480 cells were treated with maraviroc, and apoptosis-related genes were evaluated by *Human Apoptosis Panel, 96*. CP (*crossing point*) values, indicating the linear amplification of transcribed cDNA, were calculated by the *Second Derivative Maximum Method*, and the  $\Delta\Delta CT$  method was used to calculate the relative expression levels of the genes as compared to the respective untreated control samples. Averages of seven reference genes, incorporated in the panel, were used to normalize the data. **b** A schematic apoptosis pathway (*Ingenuity Pathway Analysis*) was modified to represent the modulation of signaling chain members caused by maraviroc (IC<sub>75</sub>, 48 h) in SW480 cells. For abbreviations used, see the supplementary data



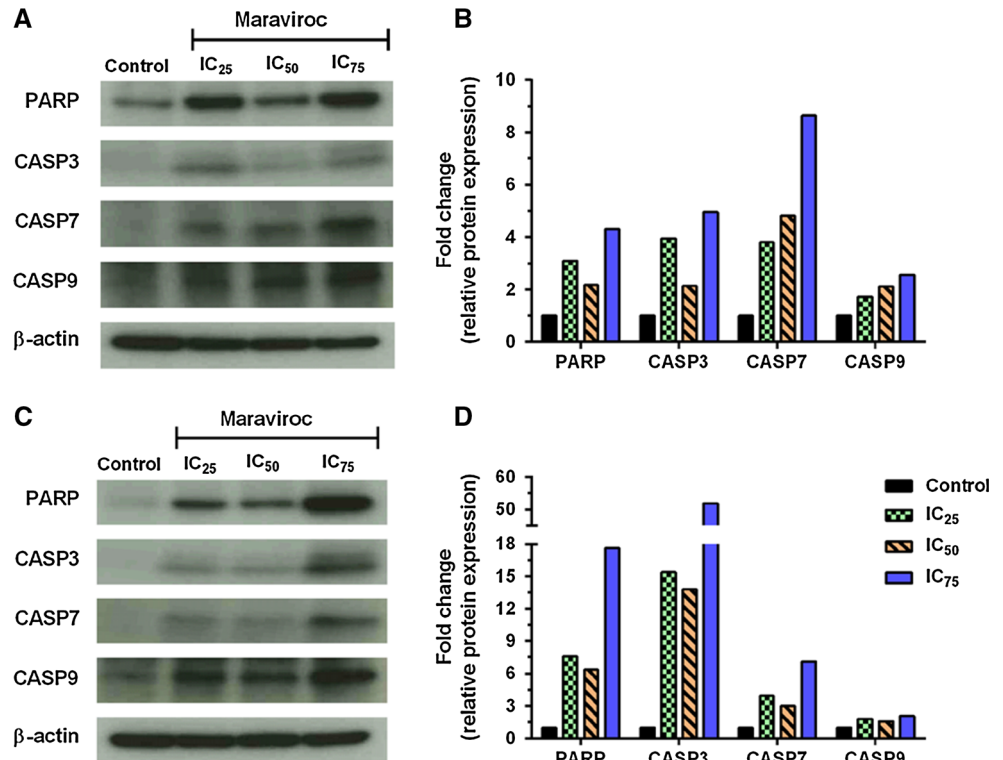
similar increases of annexin V-positive cells in both CRC cell lines. This indicates and confirmed the ability of MVC to compel the tumor cells into the apoptotic process, regardless of their primary or metastatic nature of origin.

The significant induction of apoptosis prompted us to further investigate the respective signaling pathways. For this purpose, we exposed SW480 cells with MVC and examined the apoptosis-relevant genes by a ready-made panel (see materials and methods). MVC treatment showed significant modulation ( $\geq$ twofold) of 16 genes, out of which significant proportions were comprised of the death receptors and their corresponding ligands. These included the cell surface *FAS* and tumor necrosis factor (*TNF*)

superfamily receptors. Induction of death receptors and their ligands in this study indicates the ability of MVC to induce the extrinsic arm of apoptosis in CRC cells [40]. The other two dominating groups of gene families, which were altered significantly in response to MVC exposure, were caspases and BCL2. Considerable modulations of BCL2 family members, which cover the intrinsic arm of apoptosis [41], revealed the ability of MVC to exert stress in CRC cells through mitochondrial involvement. This could occur in response to chemokine deprivation as well, which, in turn, will cause alteration of BID and subsequent activation of BAX and BAK [42]. Regarding the caspase family, we found the induction of initiator caspases (8 and



**Fig. 6** Induction of activated caspases by maraviroc exposure: Following treatment with increasing concentrations of maraviroc for 48 h, western blot analysis for the expression levels of cleaved caspases 3, 7, 9 and cleaved PARP was performed with  $\beta$ -actin as a loading control. **a, c** Maraviroc induced the expression of cleaved caspases and PARP in SW480 and SW620 cells, respectively. **b, d** Fold inductions are calculated for both cell lines by the *ImageJ Program*



10), which are required to initiate the apoptosis signaling in response to death receptor stimulation [43, 44]. The utmost induction at mRNA level was found for caspase 5 (27-fold), which is known to be involved in activation of caspase 1, which, in turn, processes the pro-inflammatory interleukins-1 $\beta$  and 18 [45].

Significant induction of initiator caspases led us to study the expressional profiles of the cleaved executor caspases (3, 7 and 9) and PARP at protein levels. Interestingly, we found a slight decrease at mRNA level of these caspases in the apoptosis panel (see pathway), but significant inductions were observed for cleaved proteins in both CRC cell lines after exposure to increasing concentrations of MVC. This indicates a high turnover of the relevant transcripts into proteins, followed by the amplification of cleaved (activated) forms for the subsequent apoptotic effects. The expression levels of cleaved caspases and PARP did not follow a concentration-dependent format for lower concentrations of MVC (IC<sub>25</sub> and IC<sub>50</sub>), which indicates a plateau of cleaved protein levels, as the differences between IC<sub>25</sub> and IC<sub>50</sub> were not significant. In addition to this, induction of cleaved proteins was also partially cell line specific, as caspase 7 was the most effectively cleaved caspase in SW480 cells, while caspase 3 was most altered in SW620 cells.

In conclusion, blocking the *CCR5* receptor by MVC induces cytotoxic and apoptotic effects in CRC cells. These antineoplastic effects were observed in CRC cells regardless of their primary or metastatic origin. These findings

led us to identify MVC as antineoplastic lead compound which can serve as proof of concept for the anticancer effects of blocking the *CCR5* receptor and will foster the development of *CCR5* antagonists for the treatment of colorectal cancer.

**Conflict of interest** None.

**References**

1. Fernandez EJ, Lolis E. Structure, function, and inhibition of chemokines. *Annu Rev Pharmacol Toxicol.* 2002;42:469–99. doi:10.1146/annurev.pharmtox.42.091901.115838.
2. Zlotnik A, Yoshie O. Chemokines: a new classification system and their role in immunity. *Immunity.* 2000;12(2):121–7.
3. Mantovani A. The chemokine system: redundancy for robust outputs. *Immunol Today.* 1999;20(6):254–7.
4. Rossi D, Zlotnik A. The biology of chemokines and their receptors. *Annu Rev Immunol.* 2000;18:217–42. doi:10.1146/annurev.immunol.18.1.217.
5. Allen SJ, Crown SE, Handel TM. Chemokine: receptor structure, interactions, and antagonism. *Annu Rev Immunol.* 2007;25: 787–820. doi:10.1146/annurev.immunol.24.021605.090529.
6. Balkwill F, Mantovani A. Inflammation and cancer: back to Virchow? *Lancet.* 2001;357(9255):539–45. doi:10.1016/S0140-6736(00)04046-0.
7. Gu L, Tseng S, Horner RM, Tam C, Loda M, Rollins BJ. Control of TH2 polarization by the chemokine monocyte chemoattractant protein-1. *Nature.* 2000;404(6776):407–11. doi:10.1038/35006097.
8. Balkwill F. Cancer and the chemokine network. *Nat Rev Cancer.* 2004;4(7):540–50. doi:10.1038/nrc1388.

9. Raman D, Sobolik-Delmaire T, Richmond A. Chemokines in health and disease. *Exp Cell Res*. 2011;317(5):575–89. doi:10.1016/j.yexcr.2011.01.005.
10. Mantovani A, Savino B, Locati M, Zammataro L, Allavena P, Bonecchi R. The chemokine system in cancer biology and therapy. *Cytokine Growth Factor Rev*. 2010;21(1):27–39. doi:10.1016/j.cytogfr.2009.11.007.
11. Lazennec G, Richmond A. Chemokines and chemokine receptors: new insights into cancer-related inflammation. *Trends Mol Med*. 2010;16(3):133–44. doi:10.1016/j.molmed.2010.01.003.
12. Raman D, Baugher PJ, Thu YM, Richmond A. Role of chemokines in tumor growth. *Cancer Lett*. 2007;256(2):137–65. doi:10.1016/j.canlet.2007.05.013.
13. Richmond A. Chemokine modulation of the tumor microenvironment. *Pigment Cell Melanoma Res*. 2010;23(3):312–3. doi:10.1111/j.1755-148X.2010.00714.x.
14. Jemal A, Bray F, Center MM, Ferlay J, Ward E, Forman D. Global cancer statistics. *CA Cancer J Clin*. 2011;61(2):69–90. doi:10.3322/caac.20107.
15. Garborg K, Holme O, Loberg M, Kalager M, Adami HO, Bretthauer M. Current status of screening for colorectal cancer. *Ann Oncol*. 2013;24(8):1963–72. doi:10.1093/annonc/mdt157.
16. Samson M, Labbe O, Mollereau C, Vassart G, Parmentier M. Molecular cloning and functional expression of a new human CC-chemokine receptor gene. *Biochemistry*. 1996;35(11):3362–7. doi:10.1021/bi952950g.
17. Raport CJ, Gosling J, Schweickart VL, Gray PW, Charo IF. Molecular cloning and functional characterization of a novel human CC chemokine receptor (CCR5) for RANTES, MIP-1-beta, and MIP-1alpha. *J Biol Chem*. 1996;271(29):17161–6.
18. Oppermann M. Chemokine receptor CCR5: insights into structure, function, and regulation. *Cell Signal*. 2004;16(11):1201–10. doi:10.1016/j.cellsig.2004.04.007.
19. New DC, Wong YH. CC chemokine receptor-coupled signalling pathways. *Acta Biochimica et Biophysica Sinica*. 2003;35(9):779–88.
20. Zimmermann T, Moehler M, Gockel I, Sgourakis GG, Biesterfeld S, Muller M, et al. Low expression of chemokine receptor CCR5 in human colorectal cancer correlates with lymphatic dissemination and reduced CD8+ T-cell infiltration. *Int J Colorectal Dis*. 2010;25(4):417–24. doi:10.1007/s00384-009-0868-y.
21. Erreni M, Bianchi P, Laghi L, Miolo M, Fabbri M, Locati M, et al. Expression of chemokines and chemokine receptors in human colon cancer. *Methods Enzymol*. 2009;460:105–21. doi:10.1016/S0076-6879(09)05205-7.
22. Schimanski CC, Moehler M, Gockel I, Zimmermann T, Lang H, Galle PR, et al. Expression of chemokine receptor CCR5 correlates with the presence of hepatic molecular metastases in K-ras positive human colorectal cancer. *J Cancer Res Clin Oncol*. 2011;137(7):1139–45. doi:10.1007/s00432-011-0980-6.
23. Weitzenfeld P, Ben-Baruch A. The chemokine system, and its CCR5 and CXCR4 receptors, as potential targets for personalized therapy in cancer. *Cancer Lett*. 2014;352(1):36–53. doi:10.1016/j.canlet.2013.10.006.
24. de Oliveira CE, Oda JM, Losi Guembarovski R, de Oliveira KB, Ariza CB, Neto JS, et al. CC chemokine receptor 5: the interface of host immunity and cancer. *Dis Markers*. 2014;2014:126954. doi:10.1155/2014/126954.
25. Chang LY, Lin YC, Mahalingam J, Huang CT, Chen TW, Kang CW, et al. Tumor-derived chemokine CCL5 enhances TGF-beta-mediated killing of CD8(+) T cells in colon cancer by T-regulatory cells. *Cancer Res*. 2012;72(5):1092–102. doi:10.1158/0008-5472.CAN-11-2493.
26. Erreni M, Mantovani A, Allavena P. Tumor-associated macrophages (TAM) and inflammation in colorectal cancer. *Cancer Microenviron*. 2011;4(2):141–54. doi:10.1007/s12307-010-0052-5.
27. Cambien B, Richard-Fiardo P, Karimjee BF, Martini V, Ferrua B, Pitard B, et al. CCL5 neutralization restricts cancer growth and potentiates the targeting of PDGFRbeta in colorectal carcinoma. *PLoS ONE*. 2011;6(12):e28842. doi:10.1371/journal.pone.0028842.
28. Ward ST, Li KK, Hepburn E, Weston CJ, Curbishley SM, Reynolds GM, et al. The effects of CCR5 inhibition on regulatory T-cell recruitment to colorectal cancer. *Br J Cancer*. 2015;112(2):319–28. doi:10.1038/bjc.2014.572.
29. Yost R, Pasquale TR, Sahloff EG. Maraviroc: a coreceptor CCR5 antagonist for management of HIV infection. *Am J Health Syst Pharm*. 2009;66(8):715–26. doi:10.2146/ajhp080206.
30. Livak KJ, Schmittgen TD. Analysis of relative gene expression data using real-time quantitative PCR and the 2(-Delta Delta C(T)) method. *Methods*. 2001;25(4):402–8. doi:10.1006/meth.2001.1262.
31. Velasco-Velazquez M, Jiao X, De La Fuente M, Pestell TG, Ertel A, Lisanti MP, et al. CCR5 antagonist blocks metastasis of basal breast cancer cells. *Cancer Res*. 2012;72(15):3839–50. doi:10.1158/0008-5472.CAN-11-3917.
32. Ochoa-Callejero L, Perez-Martinez L, Rubio-Mediavilla S, Oteo JA, Martinez A, Blanco JR. Maraviroc, a CCR5 antagonist, prevents development of hepatocellular carcinoma in a mouse model. *PLoS ONE*. 2013;8(1):e53992. doi:10.1371/journal.pone.0053992.
33. Mencarelli A, Graziosi L, Renga B, Cipriani S, D'Amore C, Francisci D, et al. CCR5 antagonism by maraviroc reduces the potential for gastric cancer cell dissemination. *Transl Oncol*. 2013;6(6):784–93.
34. Abel S, Russell D, Whitlock LA, Ridgway CE, Nedderman AN, Walker DK. Assessment of the absorption, metabolism and absolute bioavailability of maraviroc in healthy male subjects. *Br J Clin Pharmacol*. 2008;65(Suppl 1):60–7. doi:10.1111/j.1365-2125.2008.03137.x.
35. Sugimoto M, Nakamura T, Ohtani N, Hampson L, Hampson IN, Shimamoto A, et al. Regulation of CDK4 activity by a novel CDK4-binding protein, p34(SEI-1). *Genes Dev*. 1999;13(22):3027–33.
36. Sherr CJ, Roberts JM. Living with or without cyclins and cyclin-dependent kinases. *Genes Dev*. 2004;18(22):2699–711. doi:10.1101/gad.1256504.
37. Gudas JM, Payton M, Thukral S, Chen E, Bass M, Robinson MO, et al. Cyclin E2, a novel G1 cyclin that binds Cdk2 and is aberrantly expressed in human cancers. *Mol Cell Biol*. 1999;19(1):612–22.
38. Elmore S. Apoptosis: a review of programmed cell death. *Toxicol Pathol*. 2007;35(4):495–516. doi:10.1080/01926230701320337.
39. Lee SH, Meng XW, Flatten KS, Loegering DA, Kaufmann SH. Phosphatidylserine exposure during apoptosis reflects bidirectional trafficking between plasma membrane and cytoplasm. *Cell Death Differ*. 2013;20(1):64–76. doi:10.1038/cdd.2012.93.
40. Eimon PM, Kratz E, Varfolomeev E, Hymowitz SG, Stern H, Zha J, et al. Delineation of the cell-extrinsic apoptosis pathway in the zebrafish. *Cell Death Differ*. 2006;13(10):1619–30. doi:10.1038/sj.cdd.4402015.
41. Rautureau GJ, Day CL, Hinds MG. Intrinsically disordered proteins in bcl-2 regulated apoptosis. *Int J Mol Sci*. 2010;11(4):1808–24. doi:10.3390/ijms11041808.
42. Xu G, Shi Y. Apoptosis signaling pathways and lymphocyte homeostasis. *Cell Res*. 2007;17(9):759–71. doi:10.1038/cr.2007.52.
43. Chen M, Wang J. Initiator caspases in apoptosis signaling pathways. *Apoptosis*. 2002;7(4):313–9.
44. Abraham MC, Shaham S. Death without caspases, caspases without death. *Trends Cell Biol*. 2004;14(4):184–93. doi:10.1016/j.tcb.2004.03.002.
45. Denes A, Lopez-Castejon G, Brough D. Caspase-1: is IL-1 just the tip of the ICEberg? *Cell Death Dis*. 2012;3:e338. doi:10.1038/cddis.2012.86.